Measurements of geometric enhancement factors for silicon nanopillar cathodes using a scanning tunneling microscope

P. A. Lewis, B. W. Alphenaar,[a] and H. Ahmed[b]
Microelectronics Research Centre and Hitachi Cambridge Laboratory, Cavendish Laboratory, Madingley Road, Cambridge CB3 0HE, United Kingdom

(Received 11 April 2001; accepted for publication 30 June 2001)

High-density silicon nanopillar cathodes were fabricated using a self-assembling colloidal gold etch mask. Scanning tunneling microscopy experiments were performed to locate individual nanopillars and to investigate their field emission properties. Emission characteristics were obtained over a range of fixed separations from the nanopillar apex, allowing the empirical determination of the geometric field enhancement factors from the resulting Fowler–Nordheim plots. The geometric enhancement factors were found to increase dramatically for decreasing anode–cathode separation and the rate of increase is dependent on the nanopillar geometry. © *2001 American Institute of Physics.* [DOI: 10.1063/1.1396821]

Research into cathodes for vacuum microelectronics and flat panel television displays is rapidly maturing. The standard microfabricated cathodes for these applications are molybdenum Spindt tips or oxidation sharpened silicon tips. However, in order to achieve low voltage operation much research is now being done on alternative materials such as low work function diamond films[1] and nanostructured materials, including carbon nanotubes[2] and silicon nanowires.[3] One of the motivations for using nanostructures is the large geometric field enhancement factor they provide allowing for lower turn-on voltages.

So far, most measurements of electron emission from nanostructured materials have been made from emitter areas, which contain an unknown and usually large, number of emitters. It is, therefore, impossible to measure the emission characteristics of individual nanostructures and hence to determine the true effect of the geometric enhancement factor of the structure. In experiments for investigating the electron emission from surfaces, scanning probe microscopy techniques have been utilized to probe the conductivity and to measure localized emission from materials such as diamond films.[4,5] In other experiments, the standard scanning tunneling microscope (STM) work function measurement technique[6] has been modified to obtain micron-scale maps of the geometric enhancement factors of niobium surfaces.[7] However, at present measurements of emission from individual nanocathodes and the empirical determination of their geometric enhancement factor is lacking. Furthermore, for the future development of nanoscale field emission devices with anode–cathode separations <30 nm,[8] it is important to determine how the geometric enhancement factor is affected by such small separations.

In this letter, we report on the evaluation of the field emission characteristics of individual silicon nanopillars using a STM technique, which allows for the empirical determination of the geometric enhancement factors of individual nanopillars. The $I-V$ characteristics of silicon nanopillars were obtained for a range of nanopillar to anode separations and compared with results from an adjacent plane Si surface to determine the geometric enhancement factor of the nanopillars. This factor was found to increase dramatically over the nanoscale range of separations and the rate of increase was found to depend on the nanopillar geometry.

Nanopillars were fabricated, using a colloidal gold etch mask, in silicon which was doped 10^{19} cm^{-3} with phosphorous. In this process, the capping oxide was stripped with a wet etch so that only the native oxide layer remained on the silicon. Subsequently a monolayer of isolated, 30 nm diameter, colloidal gold particles was deposited on the substrate using an amino-silane adhesion agent.[9] The density of the colloids can be controlled to some extent by the time of deposition[10] and for this experiment the density was approximately 2×10^{13} colloids/m^2. Optical lithography was then used in combination with an aqua regia ($HCl:HNO_3=3:1$) wet etch to remove the colloids from half the chip.[11] Next, a $SiCl_4$ based reactive ion etch was used to form Si nanopillars with nearly vertical sidewalls,[12] which are displayed in Fig. 1(a). Aluminum ohmic contacts were made on the sides of the chip to ensure good electrical contact between the chip and the STM sample holder. Finally, a brief wet etch was

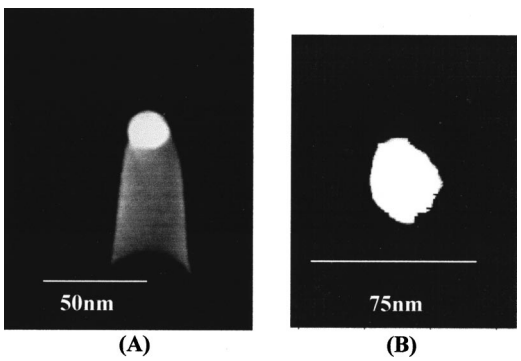

FIG. 1. (a) High magnification SEM of a silicon nanopillar with a colloidal gold cap taken at 30 kV with 35° tilt and (b) greyscale STM image of a similar nanopillar with measured diameter of >30 nm are shown.

[a]Present address: Department of Electrical and Computer Engineering, University of Louisville, Louisville, Kentucky 40292.
[b]Electronic mail: ha10@cam.ac.uk

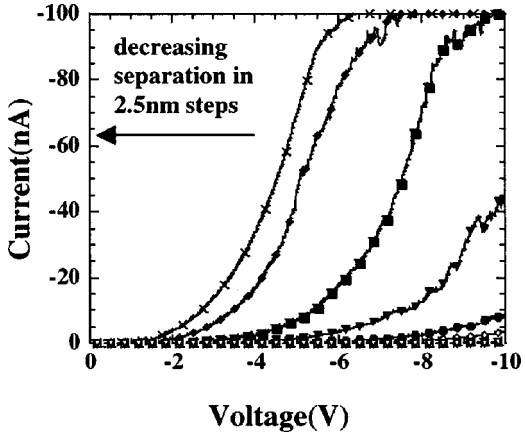

FIG. 2. Field emission $I-V$ characteristics obtained from individual silicon nanopillar over a 20 nm range of anode–cathode separations are shown. Characteristics were obtained at room temperature in an ultrahigh vacuum.

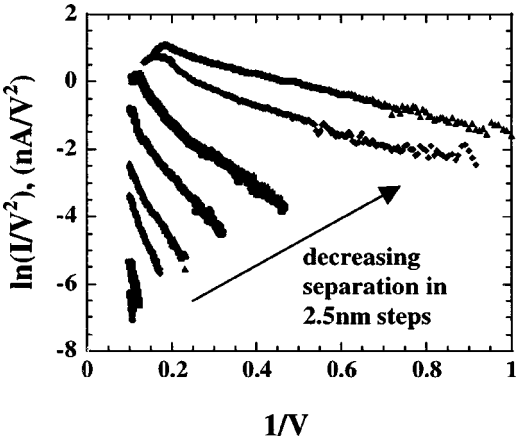

FIG. 3. F–N plots for decreasing anode–cathode separations from individual 145 nm tall silicon nanopillar are shown.

performed to remove the native oxide immediately before transferring the sample into the STM chamber, which has a base pressure of approximately 5×10^{-9} Torr.

Images and current voltage ($I-V$) characteristics were obtained with a STM in constant current mode, using electrochemically etched tungsten tips. Figure 1(b) shows a gray scale STM image of a nanopillar obtained in a constant current mode with an applied voltage of 3.0 V and current of 0.5 nA. The apparent diameter of the pillar in the image is greater than 30 nm, which is larger than the actual pillar diameter measured from the scanning electron microscopy (SEM) micrograph. The STM measures the height of the pillars to be only about 20 nm compared to the actual physical height of approximately 145 nm measured by SEM inspection. This is known to be a common difficulty when imaging high aspect ratio structures with STM[13,14] because of the problems associated with the STM tip convolution with pillar shape and the inability of the STM tip to penetrate in between pillars. The separation between pillars for this sample ranges from approximately 100 nm to several hundred nanometers.

The procedure for obtaining the emission characteristics is as follows: first, an image of a pillar is obtained and the STM tip is centered above the pillar. Then, the tip is withdrawn from the pillar and the feedback is disconnected so that $I-V$ characteristics can be obtained at fixed locations. The STM tip is then advanced in 2.5 nm steps and at each location an average of 16 $I-V$ sweeps is recorded. For the measurements, the potential applied to the substrate was swept from 0 to–10 V with the STM tip grounded. The distance between the pillar and STM tip is determined by contacting the STM tip to the pillar at the final stage of the experiments. When $I-V$ measurements were taken without contacting the pillar, it was possible to reobtain an image of the nanopillar afterwards. However, after contact, images of the same pillar were difficult to reobtain.

Figure 2 displays a typical set of emission characteristics from an individual silicon nanopillar with a colloidal gold top. Figure 2 shows that, as expected, the turn-on voltage for the nanopillar decreases as the anode (STM tip)–cathode (nanopillar) separation decreases. Measurements were also made at various distances from the flat region of the chip without nanopillars. The $I-V$ sweeps from the flat region only show turn on for less than 10 V when the STM tip is less than 5 nm from the surface. Field emission characteristics were obtainable at under 10 V for separations greater than 20 nm, which corresponds to greater than 165 nm from the nanopillar base. This is clear evidence of emission due to the presence of the nanopillar rather than from the normal substrate surface.

In standard Fowler–Nordheim (F–N) theory, the emission current is a function of the work function (φ), voltage (V), voltage conversion factor (β), and emission area (α) and is given by[15]

$$I = aV^2 \exp[-b/V)] \quad \text{amps/cm}^2, \tag{1}$$

where $a = A\alpha\beta^2(1.1\phi)^{-1}\exp[1.14\times10^{-7}(B\varphi^{-1/2})]$, $b = 0.95\phi^{3/2}B/\beta$, $A = 1.54\times10^{-6}$ and $B = 6.87\times10^{7}$. The voltage conversion factor β is the proportionality factor between the applied voltage and the electric field (E) at the cathode apex, $E=\beta V$. β can be split into two components, $\beta = g/d$, so as to separate the geometric enhancement factor (g) from the anode–cathode separation (d). For a flat anode and cathode, the geometric enhancement factor is one and the density of the equipotential surfaces is constant between the anode and cathode. The geometric enhancement factor arises from the compression of the equipotential surfaces around a protrusion on the cathode that leads to the maximum electric field being at the apex of the protrusion.

From our experiments, we determine the geometric enhancement factor by extracting the voltage conversion factors from the F–N plots of the data. A manipulation of Eq. (1) yields $\ln(I/V^2) = -b(1/V) + \ln(a)$. Thus, assuming the work function of the colloidal gold is 4.8 eV, we can calculate the voltage conversion factors from the slopes of the linear fits to the F–N plots for every separation. Since the separation between the nanopillar base and the STM tip is measured, we can then estimate the geometric enhancement factor of the nanopillars by multiplying β by the separation.

Figure 3 displays the F–N plots for the $I-V$ characteristics at different separations. As the separation between the anode and nanopillar decreases, the slope of the F–N plots decreases. This general trend is expected because the slope is inversely proportional to the voltage conversion factor, which increases with decreasing anode–cathode separation.

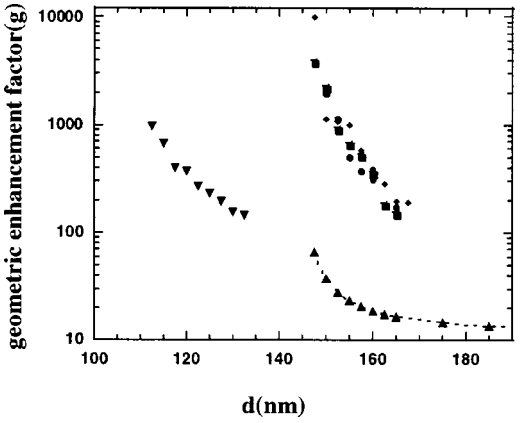

FIG. 4. Log plots of empirically determined geometric enhancement factors vs anode–cathode separation (d), where d is the distance from the pillar base to the STM tip, for 145 nm tall nanopillars (■, ●, and ◆), and 110 nm tall nanopillar (▼) are shown. Finite element calculations for 145 nm tall nanopillars (▲) are presented.

However, contrary to the usual models assuming that g is independent of the separation, the values of g we extract from the plot are strongly dependent on d. This is illustrated in Fig. 4 which displays a log plot of the extracted values of g vs d, where d is the separation from the pillar base to the STM tip. The plot contains three sets of data obtained from nanopillars on the same sample, showing that while the values might vary slightly the trend is reproducible.

The values of the geometric enhancement factor range from approximately 150 for the largest separations to greater than a thousand for the smallest separations. Data from a second sample with nanopillars approximately 110 nm tall and <30 nm in diameter are also plotted. The lower aspect ratio pillar does not achieve as high a value of enhancement factors, but g still displays a strong dependence on d. For comparison, enhancement factors from the flat region of the sample were also measured, and were determined to be only approximately 10, and independent of d. This means that the large geometric enhancement factors shown in Fig. 4 can be directly attributed to the nanopillars, and are not due to the STM tip.

A standard estimation of the geometric enhancement factor is based on the rounded whisker model,[16] which assumes a cylinder with a hemispherical top protruding from a flat plane, where the separation d is defined as the distance from the base of the cylinder to the anode. The geometric enhancement factor at the pillar apex is $g=h/r+3$, where h and r are the height and radius of the nanopillar, respectively. Using this model, the enhancement factor for a 145 nm tall nanopillar is approximately 15. The experimental values of g for the largest separations are almost an order of magnitude greater than this value, and continue to deviate from the model for decreasing separations. Clearly, a more detailed model is needed to explain the geometric enhancement factor for nanometer scale pillars.

To account for the separation dependence, we have performed a calculation of the electric field between the pillar and a flat anode using a three-dimensional finite element model. The geometric enhancement factors (g) are subsequently obtained by $g=Ed/V$, where E is the electric field at the pillar apex, d is the distance from the nanopillar base to the anode, and V is the applied voltage. The geometric enhancement factors calculated using this model for 30 nm diameter and 145 nm tall pillars with hemispherical tops are shown as a dashed line in Fig. 4. For large separations, the geometric enhancement factor remains approximately constant at about 10, but below 185 nm separations (d) when the anode to nanopillar apex distance is <40 nm, there is a sharp increase to a value greater than 60.

Qualitatively then, the finite element method accounts for the strong separation dependence in g observed in our experiments, however, the calculated geometric enhancement factors are still far lower than the experimentally determined values. One possible explanation for this quantitative difference is the existence of small protrusions on the surface of the nanopillar, which can form through the surface roughening and material redeposition of the dry etching process. We can approximate the influence of this effect by multiplying the geometric enhancement factor of the cathode by the aspect ratio of the nanoprotrusion.[17] If the aspect ratio of the protrusions is greater than 10, they could further increase the geometric enhancement by an order of magnitude, which gives better agreement with our experimental results. Further measurements of pillars with a variety of different surface conditions are needed to test this hypothesis.

In conclusion, we have characterized electron emission from individual silicon nanopillar cathodes using a STM tip as an anode to obtain $I-V$ characteristics over a range of decreasing anode–cathode separations. We have found that for the nanoscale separations in these experiments, the geometric enhancement factor is strongly dependent on the separation. The electric field at the nanocathodes apex increases much faster than calculated from standard assumptions and the rate of increase depends on the cathode geometry.

[1] W. Zhu, G. P. Kochanski, and S. Jin, Science **282**, 1471 (1998).
[2] W. A. de Heer, A. Chatelain, and D. Ugarte, Science **270**, 1179 (1995).
[3] F. C. K. Au, K. W. Wong, Y. H. Tang, Y. F. Zhang, I. Bello, and S. T. Lee, Appl. Phys. Lett. **75**, 1700 (1999).
[4] T. Inoue, D. F. Ogletree, and M. Salmeron, Appl. Phys. Lett. **76**, 2961 (2000).
[5] I. Andrienko, A. Cimmino, D. Hoxley, S. Prawer, and R. Kalish, Appl. Phys. Lett. **77**, 1221 (2000).
[6] G. Binnig, N. Garcia, H. Rohrer, J. M. Soler, and F. Flores, Phys. Rev. B **30**, 4816 (1984).
[7] P. Niedermann, C. Renner, A. Kent, and O. Fischer, J. Vac. Sci. Technol. A **8**, 594 (1990).
[8] A. A. G. Driskill-Smith, D. G. Hasko, and H. Ahmed, Appl. Phys. Lett. **75**, 2845 (1999).
[9] T. Sato, D. G. Hasko, and H. Ahmed, J. Vac. Sci. Technol. B **15**, 1 (1997).
[10] K. C. Grabar, P. C. Smith, M. D. Musick, J. A. Davis, D. G. Walter, M. A. Jackson, A. P. Guthrie, and M. J. Natan, J. Am. Chem. Soc. **118**, 1148 (1996).
[11] P. A. Lewis and H. Ahmed, J. Vac. Sci. Technol. B **17**, 3239 (1999).
[12] P. A. Lewis, H. Ahmed, and T. Sato, J. Vac. Sci. Technol. B **16**, 2938 (1998).
[13] J. K. Gimzewski, A. Humbert, J. G. Bednorz, and B. Reihl, Phys. Rev. Lett. **55**, 951 (1985).
[14] J. M. Gomez-Rodriguez, L. Vazquez, A. Bartolome, and A. M. Baro, Ultramicroscopy **30**, 355 (1989).
[15] I. Brodie and C. A. Spindt, Adv. Electron. Electron Phys. **83**, 1 (1992).
[16] T. Utsumi, IEEE Trans. Electron Devices **38**, 2276 (1991).
[17] V. V. Zhrinov, E. I. Givargizov, and P. S. Plekhanov, J. Vac. Sci. Technol. B **13**, 418 (1995).